# Supporting Information

## Chemical-doping-driven crossover from graphene to "ordinary metal" in epitaxial graphene grown on SiC

Chiashain Chuang[1,2,3], Yanfei Yang[1,4], Sujitra Pookpanratana[1], Christina A. Hacker[1], Chi-Te Liang[2,5*], Randolph E. Elmquist[1*]

[1] *National Institute of Standards and Technology (NIST), Gaithersburg, MD 20899, USA.*

[2]*Department of Physics, National Taiwan University, Taipei 106, Taiwan*

[3]*Division of Materials Science, Graduate School of Engineering, Chiba University, Chiba 263-8522, Japan*

[4]*Joint Quantum Institute, University of Maryland, College Park, MD 20742, USA*

[5]*Department of Physics, Stanford University, Stanford, CA 94305, USA*

E-mail: ctliang@phys.ntu.edu.twandrandolph.elmquist@nist.gov

**Content**

## Supplementary Information 1: Low-temperature vacuum annealing, cool-down and measurements at 1.5 K

The key to this work is to perform low-temperature gentle heating in vacuum. Figure S1 shows a schematic diagram of the top-loading probe, the sample and its holder, and the electrical wiring as well as the wiring for gently heating the device.

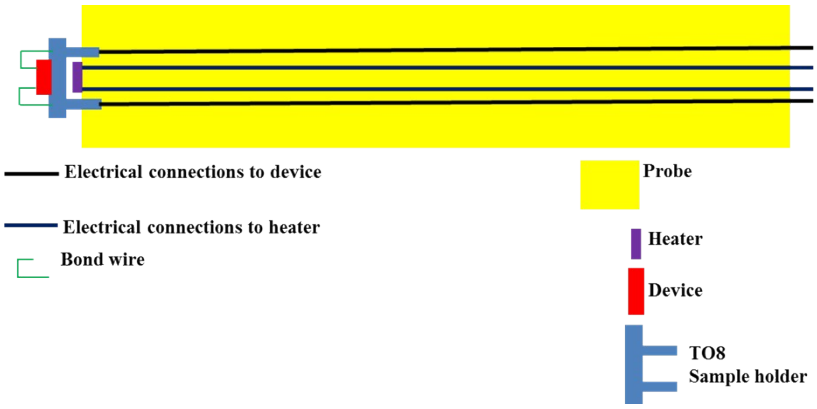


Figure S1 A schematic diagram showing the top-loading probe, sample and its TO8 holder and electrical wiring.

The following schematic diagrams show various procedures for performing our measurements.

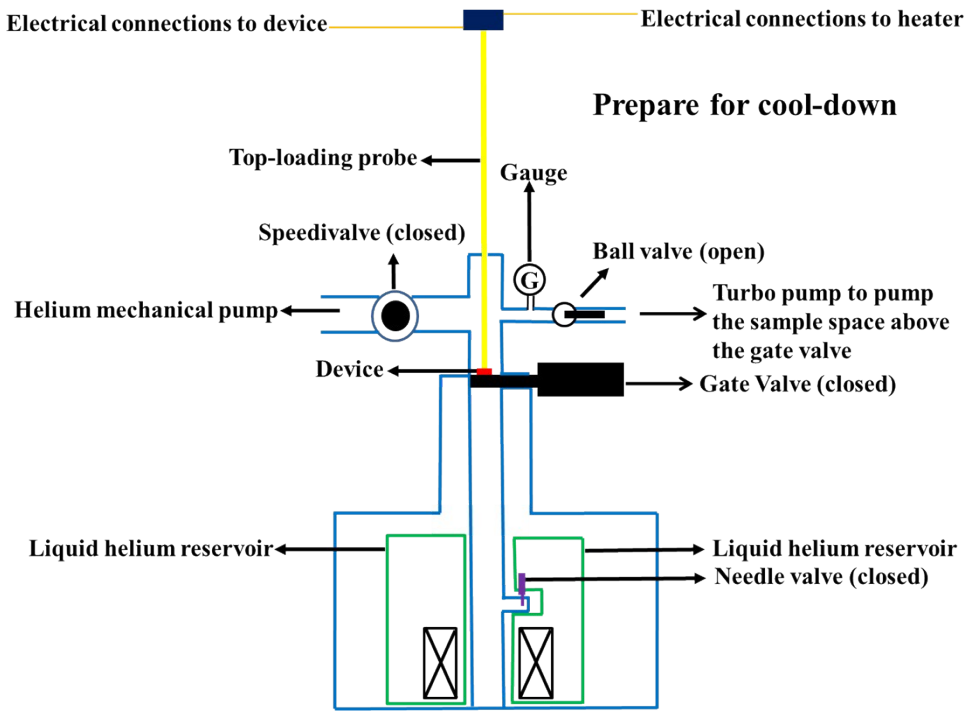


Figure S2: Set-up for preparing to cool-down the device.

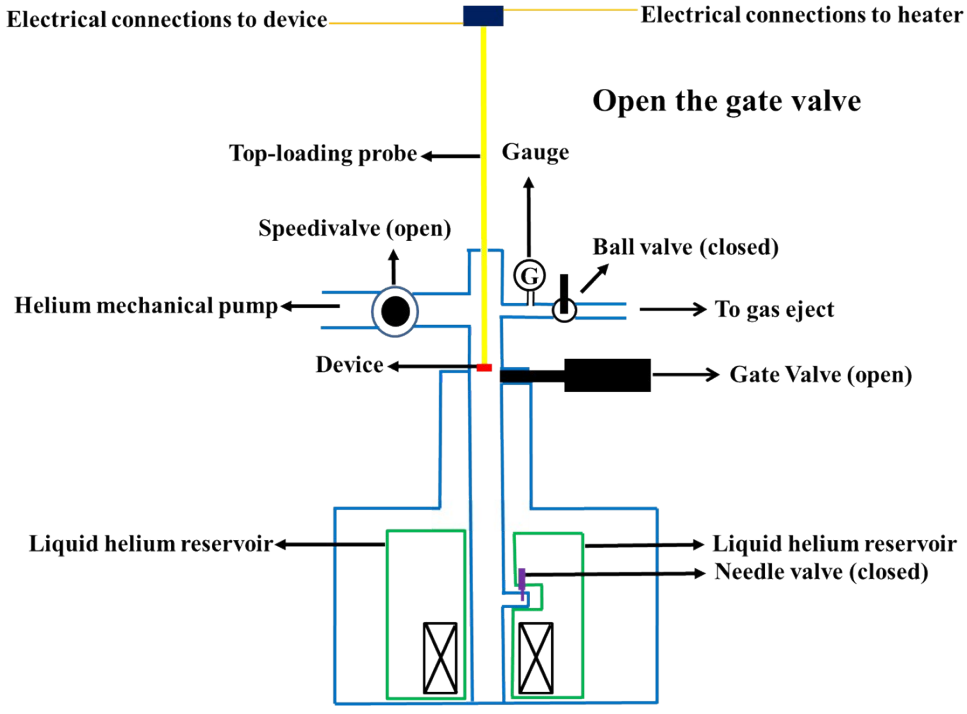


Figure S3 Open the gate valve and close the ball valve before lowering the probe

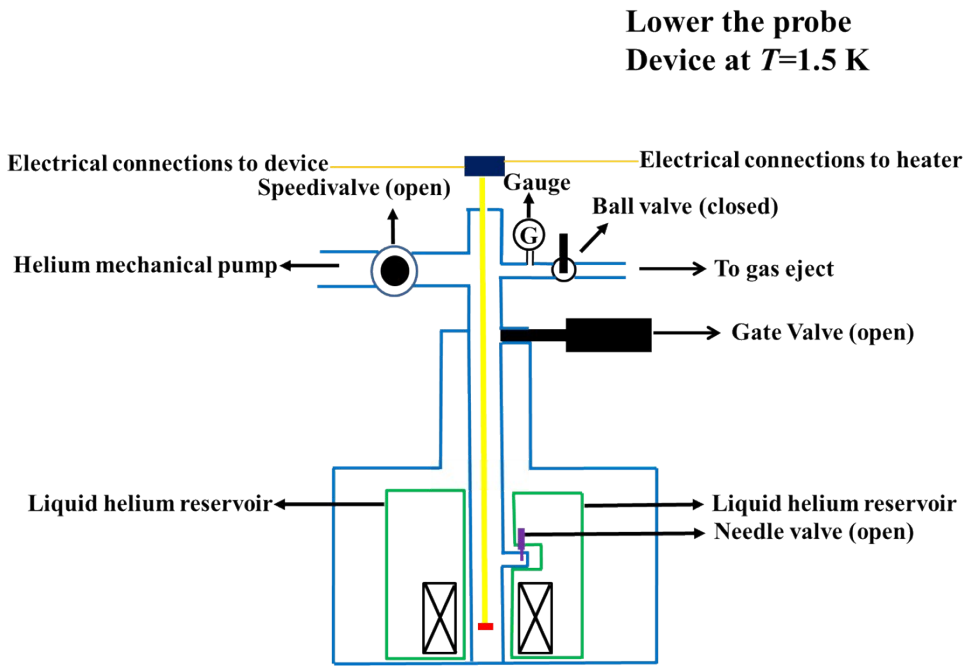


Figure S4 Lowering the probe so that the device is at 1.5 K

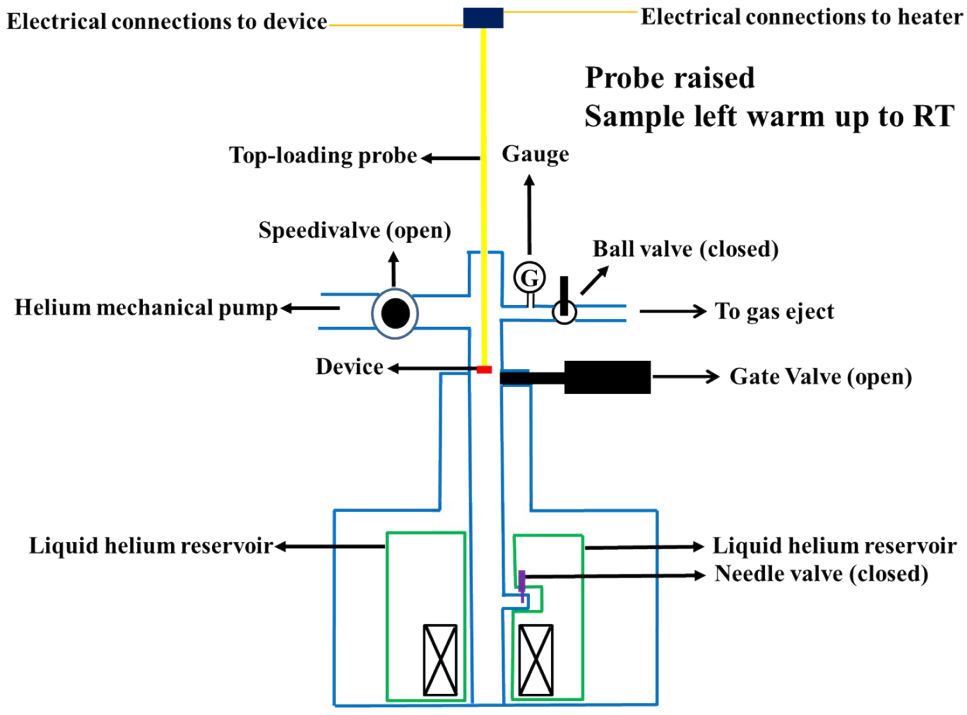


Figure S5 Raising the probe so that the device is left to warm up to room temperature

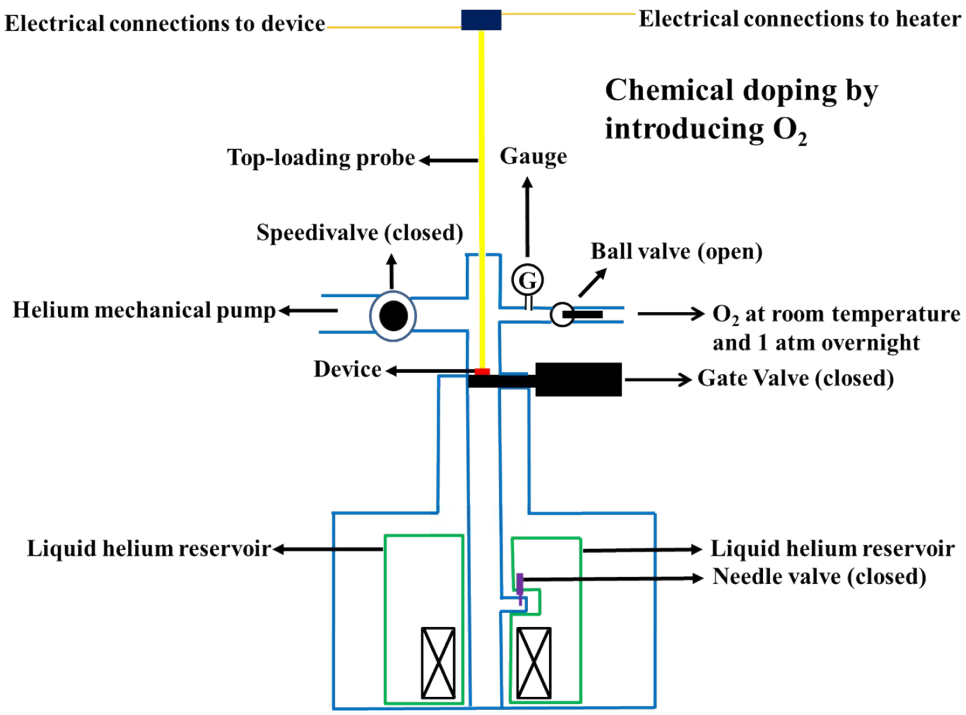


Figure S6 Set-up for introducing $O_2$ doping.

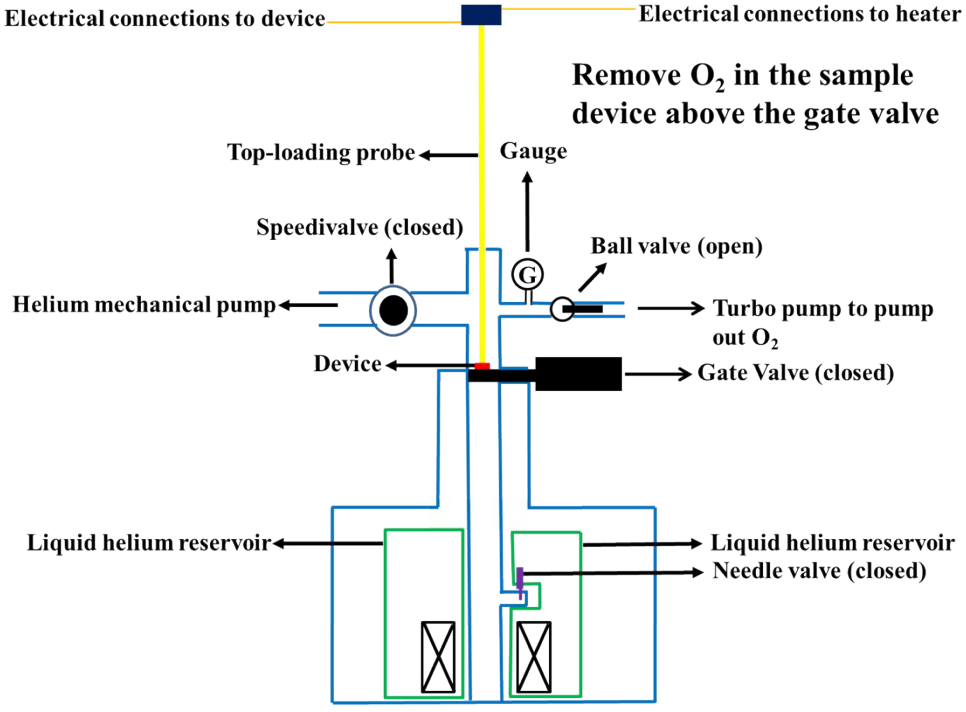


Figure S7 Set-up for finishing $O_2$ doping before cool-down.

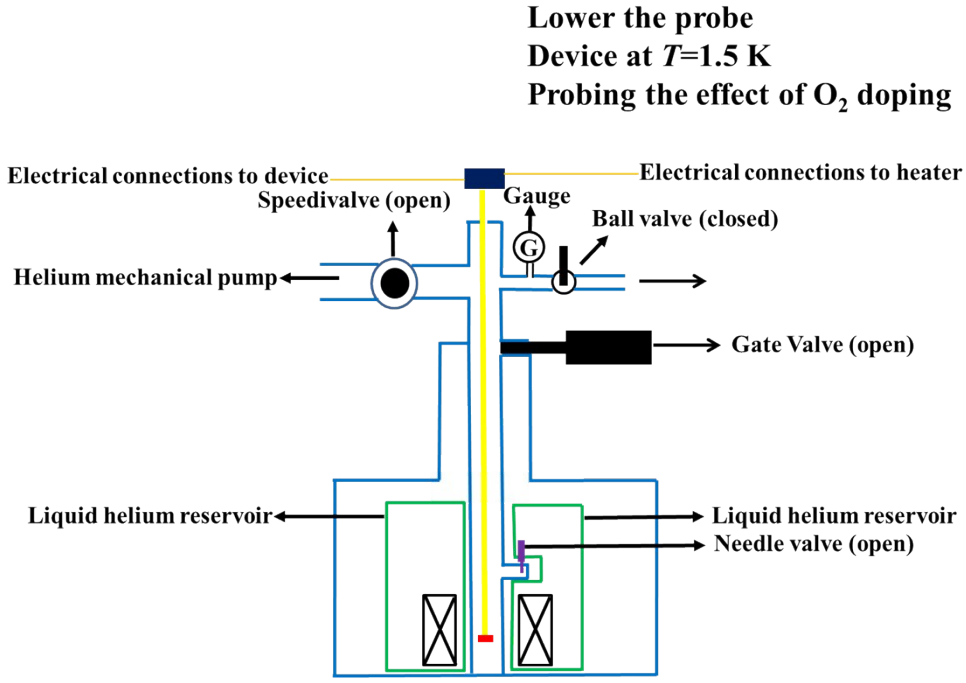


Figure S8 Probing the effect of $O_2$ doping by measurements at 1.5 K.

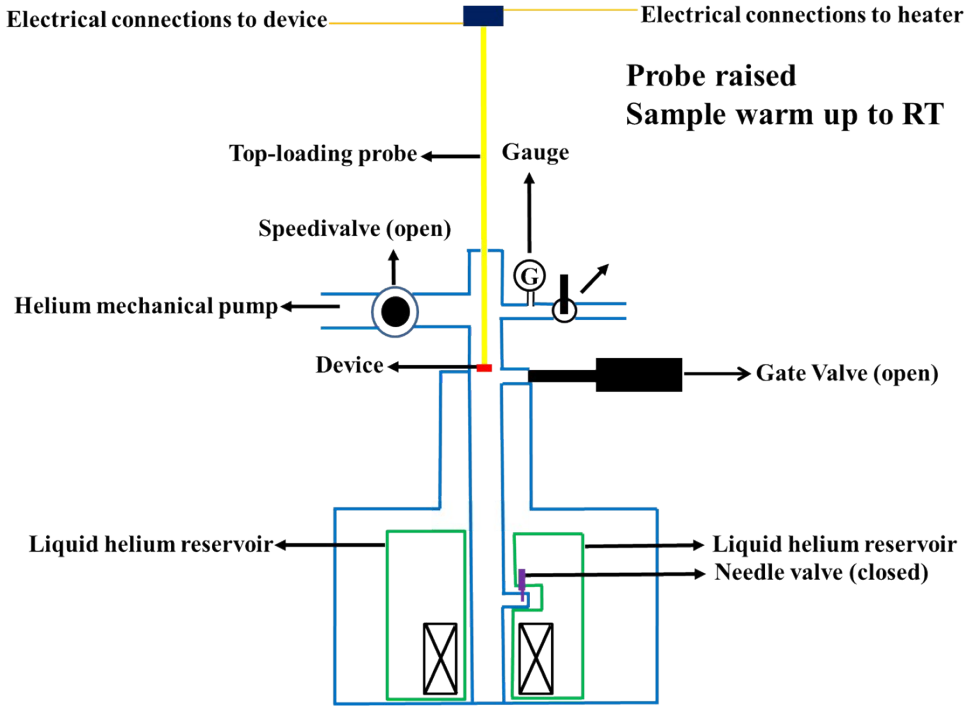


Figure S9 Once low-temperature measurements had been completed, the probe was raised and the device was left to warm up overnight.

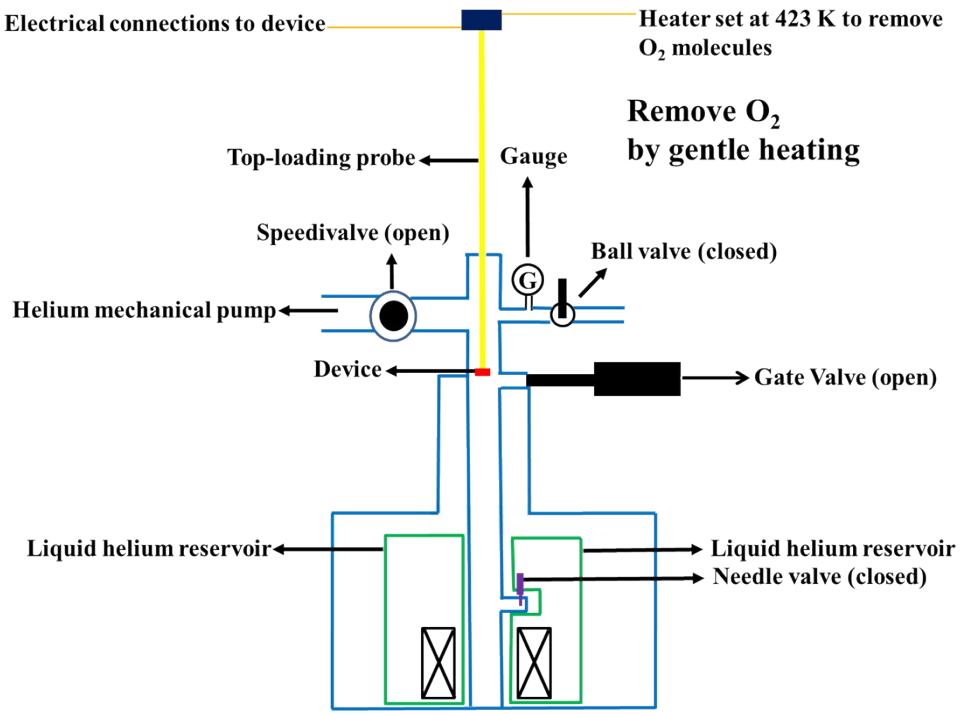


Figure S10 Set-up for removing $O_2$ molecules by gently heating the device to 423 K.

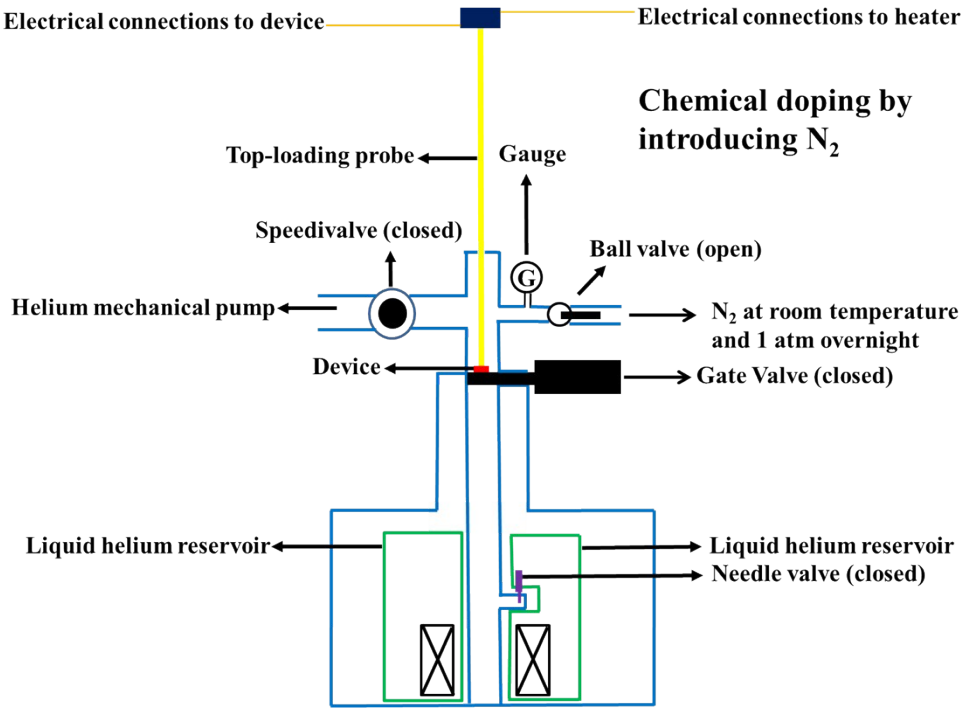


Figure S11 Once $O_2$ molecules had been removed by gently heating the device under low helium pressure, $N_2$ (or other gases) doping can be introduced.

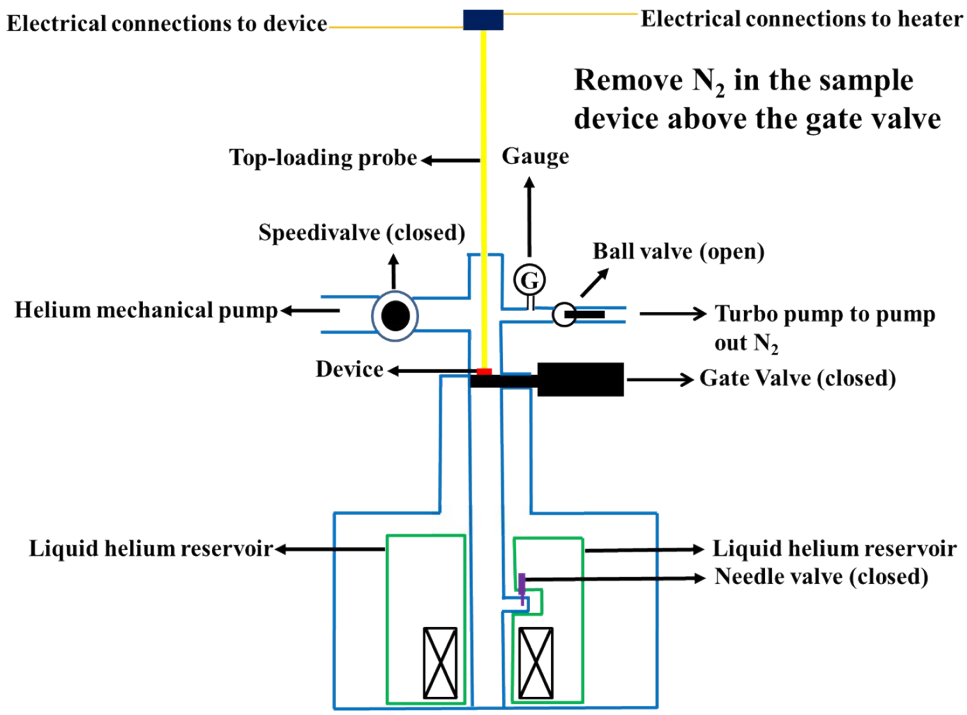


Figure S12 Set-up for removing $N_2$ above the gate valve before cooling down the device.

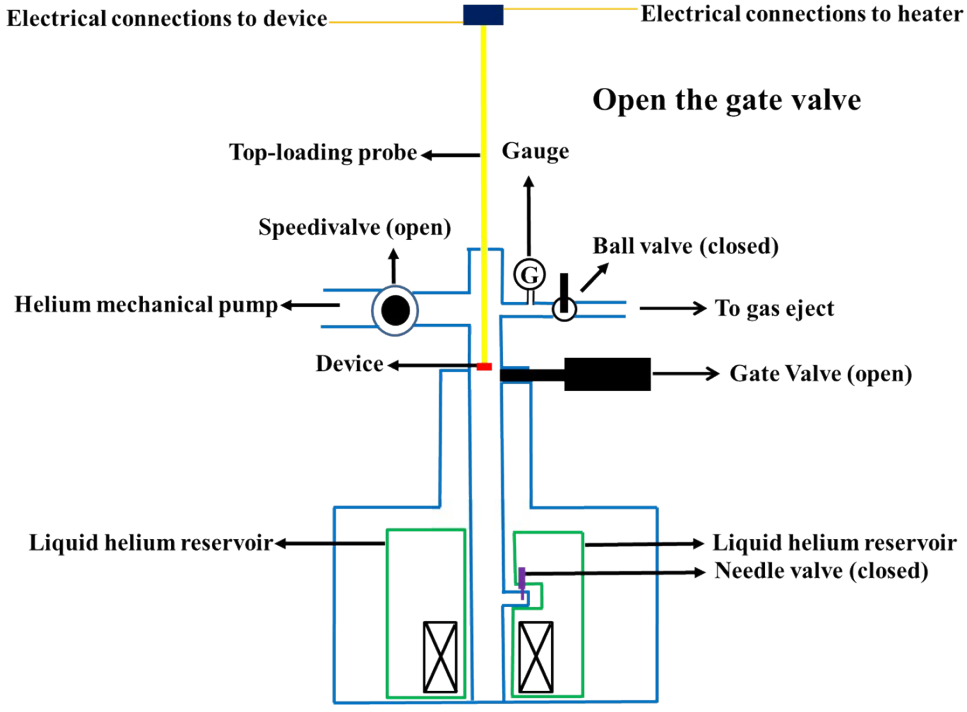


Figure S13 Open the gate valve and close the ball valve before cooling down the device.

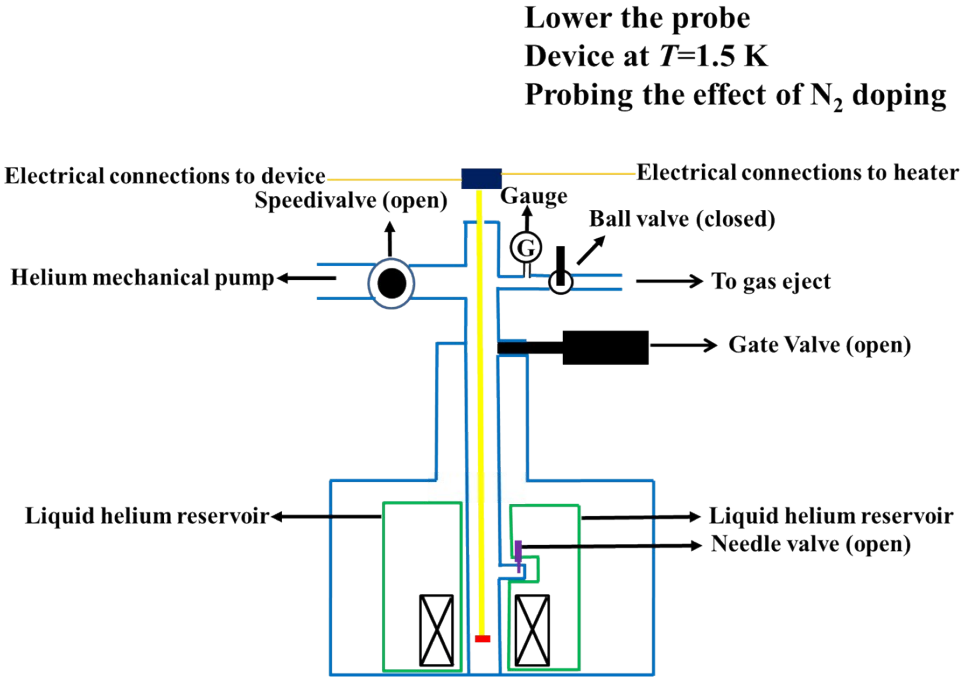


Figure S14 Cooling down the device to 1.5 K to probe the effect of $N_2$ doping.

## Supplementary Information 2: The influence of selective chemical doping

In order to know what gases from air can decrease the carrier density in graphene on SiC so as to gradually form the $\nu = 2$ quantum Hall plateau, we respectively exposed $N_2$, $O_2$, $H_2O$ vapor, $CO_2$ and air in one atmosphere into our vacuum chamber overnight (around 17 hours) after vacuum annealing at 150 ºC in 5 minutes to clean original adsorbates from air so as to form new adsorbates on graphene. Figure S1 (a) shows the SdH oscillations for $N_2$, $O_2$, $H_2O$ vapor, $CO_2$, air and original magneto-resistivity after vacuum annealing at 150 ºC in 5 minutes, which is highly reproducible as shown in the inset of Fig. S1 (a) for this heating process. (The maximal carrier density variable range for each heating process is around $2\times10^{11}$ $cm^{-2}$ and the maximal classical Drude mobility variable range is around 200 $cm^2V^{-1}s^{-1}$.) For $N_2$ and $CO_2$ exposure, the $\rho_{xx}$ in SdH oscillations and the $R_{xy}$ are similar to the magneto-resistivity after vacuum annealing at 150 ºC in 5 minutes as shown in Fig. S15 (a) and Fig. S15 (b). Also, the carrier density $n$, classical Drude mobility $\mu_t$, quantum mobility $\mu_q$ and the ratio for $\mu_t/\mu_q$ are close to the same value as listed in table 1, which implies that the $N_2$ and $CO_2$ from air are not the key gases to affect the chemical doping in the SiC graphene devices so as to change the transport property.

However, the magneto-resistivity in $\rho_{xx}$ and $R_{xy}$ for $O_2$, $H_2O$ and air change obviously as shown in Fig. S15 (a) and Fig. S15 (b). Especially, the quantum Hall plateau for $\nu = 6$ in $O_2$ and air gradually raised up and the quantum Hall plateau for $\nu = 2$ in $H_2O$ vapor appeared in high field regime as shown in Fig. S15 (b), which suggested that the $O_2$ and $H_2O$ from air are the key gases adsorbed on graphene to affect the chemical doping to transform into the precise and wide quantum Hall plateau for $\nu = 2$ from $\nu = 6$ [1-7]. Most importantly, the related carrier densities all decreased due to charge transfer or neutralize the charged impurities within graphne/SiC substrate in comparison with one for the heating process as listed in table 1 so as to increase the $\mu_t$ and $\mu_q$, which was supported by previous reports[1-8].

(a) (b)

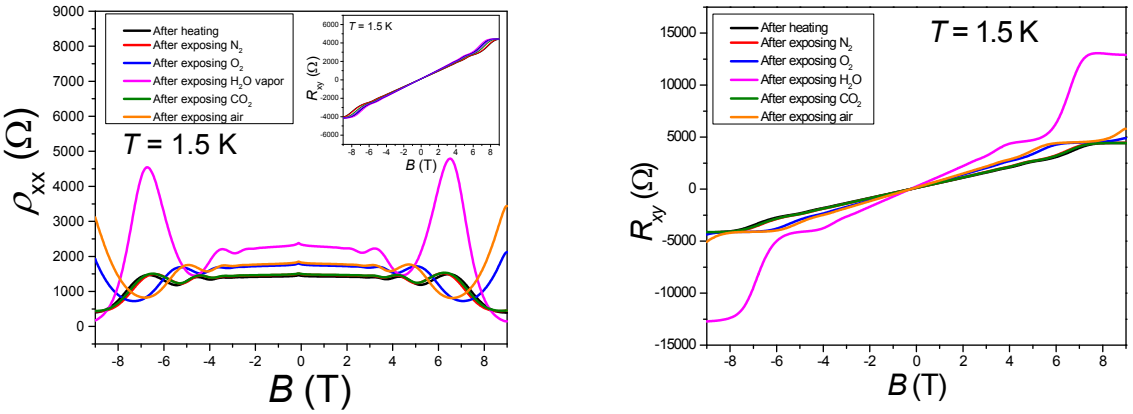


Fig. S15. The magneto-resistivity changedue to chemical doping after exposing the device to various gases ($N_2$, $O_2$, $H_2O$ Vapor, $CO_2$ and air) at one atmosphere. Before each exposure, the sample was heating in vacuum at 423 K in 5 minutes. (a) The longitudinal resistivity $\rho_{xx}$ at $T = 1.5$ K. The inset shows the reproducibility in Hall resistance $R_{xy}$ after cleaning the adsorbed gases that were from exposing gases overnight on the low-carrier density graphene. (b) The Hall resistance $R_{xy}$ at $T = 1.5$ K.

| | $n$ $10^{11}cm^{-2}$ | $\mu_t$ ($cm^2/vs$) | $\mu_q$ ($cm^2/vs$) | $\mu_t/\mu_q = \tau_t/\tau_q$ |
|---|---|---|---|---|
| Heating | 12.94 | 3303 | 1513 | 2.18 |
| $N_2$ | 12.46 | 3324 | 1498 | 2.22 |
| $O_2$ | 10.17 | 3416 | 1663 | 2.05 |
| $H_2O$ | 6.46 | 4065 | 2057 | 1.98 |
| $CO_2$ | 12.57 | 3283 | 1479 | 2.22 |
| Air | 9.49 | 3559 | 1742 | 2.04 |

Table S1. The carrier density $n$, the transport mobility $\mu_t$, the quantum mobility $\mu_q$ and the ratio for transport mobility to quantum mobility $\mu_t/\mu_q$ with different gases exposure conditions.

## Supplementary Information 3: The effective mass and quantum mobility calculations from Shubnikov-de Haas oscillations

In order to calculate the effective mass $m^*$ of the carriers and quantum mobility $\mu_q$ in the graphene device, we analyzed the amplitudes of the SdH oscillations at different temperatures and magnetic fields. The amplitudes of the SdH oscillations $\rho_{xx}$ is described by Ref. 9, 10:

$$\Delta\rho_{xx}(B;T) = 4\rho_0 exp\left[\frac{-\pi}{\mu_q B}\right] D(B,T) \quad (1)$$

where $D(B, T) = \frac{4\pi^3 k_B m^* T}{heB} / sinh(\frac{4\pi^3 k_B m^* T}{heB})$, $k_B$, $h$, $\mu_q$, $e$ and $\rho_0$, are the Blotzmann constant, Planck constant, quantum mobility, electron charge and the resistivity at zero magnetic field, respectively. The inset of Fig. S16(a) shows the amplitudes of the SdH oscillations at a fixed magnetic field of $B$ = 5.23 T. According to the well fitted

experimental results in equation 1 as shown in Fig. S16(a), the measured effective mass in the single layer epitaxial graphene is around 0.033 $m_e$ ($m_e$ is the rest mass of an electron), which is larger than the zero effective mass in Dirac cone due to the higher carrier density. From the effective mass $m^*$ = 0.033 $m_e$, we are able to calculate quantum mobility $\mu_q \approx 1512$ $cm^2V^{-1}s^{-1}$ as shown in Fig. S16(b) by analyzing the amplitudes of the longitudinal resistivity oscillations versus the inverse of $B$ at $T$ = 1.5 K.

(a) (b)

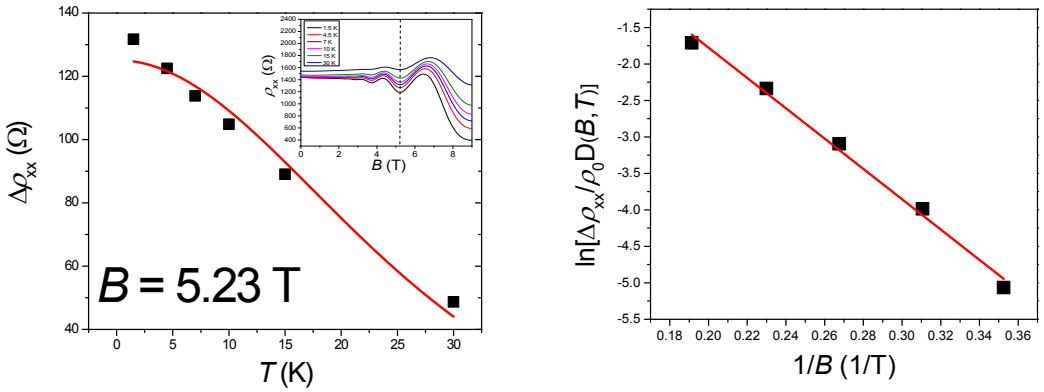


FigureS16 (a) The amplitudes of the measured oscillations $\Delta\rho_{xx}$ at $B$ = 5.23 T at different temperatures. The inset shows the valley of Shubnikov-de Haas oscillations at $B$ = 5.23 T. (b) $\ln\left[\frac{\Delta\rho_{xx}}{\rho_0 D[B,T]}\right]$ as a function of the inverse measured magnetic field $1/B$ at $T$ = 1.5 K.

## Supporting Information References


1 F.Schedin, A. K. Geim,S. V. Morozov, E. W. Hill, P. Blake, M. I. Katsnelson and K. S. Novoselov, *Nat. Mater.* 2007, **6**, 652-5.

2 Y. Yang, K. Brenner and R. Murali,*Carbon*2012, **50,** 1727-33.

3 Z. H. Ni, H. M. Wang, Z. Q. Luo, Y. Y. Wang, T. Yu, Y. H. Wu and Z. X. Shen,*J. Raman Spectrosc.*2010, **41**, 479-83.

4 P. L. Levesque, S. S. Sabri,C. M. Aquirre, J. Guillemette, M. Siaj, P. Desjardins, T. Szkopek and R. Matel, *Nano Lett.*2010, **11**, 132-7.

5 S. Ryu, L. Liu, S. Berciaud, Y.-J. Yu, H. Liu, P. Kim, G.W. Flynn and L. E. Brus, *Nano Lett.* 2010, **10**, 4944-51.

6 H. Liu,Y. Liu andD.Zhu,*J. Mater. Chem.*,2011,**21**, 3335-45.

7 H. Wang,Y.Wu, C. Cong,J. Shang andT. Yu,*ACS Nano*,2010, **4**, 7221-8.

8 E. H. Hwang andS. Das Sarma,*Phys. Rev. B*,2008, **77**,195412.

9 P. T.Coleridge,R. Stoner andR. Fletcher,*Phys. Rev. B*1989, **39**, 1120-4.

10 C. Chuang, L.-H. Lin, N. Aoki, T. Ouchi, A. M. Mahjoub,T.-P. Woo, J. P. Bird,Y. Ochiai, S.-T. Lo, C.-T. Liang,*Nanoscale Res. Lett.*2013, **8**, 214.